Assessment of the validity of a log-law for wall-bounded turbulent bubbly flows

Bragg, A.; Liao, Y.; Fröhlich, J.; Ma, T.;

Originally published:

September 2021

International Journal of Heat and Fluid Flow 91(2021), 108857

DOI: https://doi.org/10.1016/j.ijheatfluidflow.2021.108857

Assessment of the validity of a log-law for wall-bounded turbulent bubbly flows

Andrew D. Bragg[a], Yixiang Liao[b], Jochen Fröhlich[c], Tian Ma[a,b,*]

[a] *Department of Civil and Environmental Engineering, Duke University, Durham, NC 27708, USA*
[b] *Helmholtz-Zentrum Dresden - Rossendorf, Institute of Fluid Dynamics, Bautzner Landstrasse 400, 01328 Dresden, Germany*
[c] *Technische Universität Dresden, Institute of Fluid Mechanics, 01062 Dresden, Germany*

Abstract

There has been considerable discussion in recent years concerning whether a log-law exists for wall-bounded, turbulent bubbly flows. Previous studies have argued for the existence of such a log-law, with a modified von Kármán constant, and this is used in various modelling studies. We provide a critique of this idea, and present several theoretical reasons why a log-law need not be expected in general for wall-bounded, turbulent bubbly flows. We then demonstrate using recent data from interface-resolving Direct Numerical Simulations that when the bubbles make a significant contribution to the channel flow dynamics, the mean flow profile of the fluid can deviate significantly from the log-law behaviour that approximately holds for the single-phase case. The departures are not surprising and the basic reason for them is simple, namely that for bubbly flows, the mean flow is affected by a number of additional dynamical parameters, such as the void fraction, that do not play a role for the single-phase case. As a result, the inner/outer asymptotic regimes that form the basis of the derivation of the log-law for single-phase flow do not exist in general for bubbly turbulent flows. Nevertheless, we do find that for some cases, the bubbles do not cause significant departures from the unladen log-law behaviour. Moreover, we show that if departures occur these cannot be understood simply in terms

*Corresponding author
Email address: tian.ma@hzdr.de (Tian Ma)

of the averaged void fraction, but that more subtle effects such as the bubble Reynolds number and the competition between the wall-induced turbulence and the bubble-induced turbulence must play a role.

Keywords: bubbly flow, log-law, wall-bounded turbulent flows

1. Introduction

In engineering calculations of wall-bounded turbulent liquid flows containing bubbles [1], a quantity of key interest is the mean liquid velocity $\overline{\mathbf{u}}$, where $\mathbf{u}$ is the instantaneous liquid velocity field, and the overbar denotes statistical averaging. This quantity is often determined using an Euler-Euler (EE), Reynolds-averaged framework with the Reynolds stresses appearing in the equation for $\overline{\mathbf{u}}$. In most cases these are modelled with a two-equation eddy viscosity closure [2, 3], so that the main unknowns are the mean velocity $\overline{\mathbf{u}}$, the mean pressure $\overline{p}$, the average void fraction α, and the two quantities describing the properties of the turbulent liquid, k and ε or ω, for example. In the present study we focus on fully developed bubbly flow along a vertical wall.

Compared to the single-phase flow, the presence of bubbles has the following main effects in this framework. First, the mixture density is altered, so that the momentum transport via advection is altered. With the fully developed parallel flows considered below this can be neglected. Second, due to the gravity force depending on the mixture density, i. e. the void fraction, a driving term additional to the pressure gradient occurs – favourable or unfavourable, depending on the direction of the flow. The distribution of the void fraction in wall-normal direction depends on the detailed properties of the dispersed bubbles, such as deformability [4], as well as the turbulent flow of the continuous phase, related to the Reynolds number, for example [5]. Near-wall peaks of the void fraction can be observed, as well as near-wall depletion [6, 7], but also relatively uniform distribution [8].

The third effect is that bubbles due to their relative velocity with respect to the liquid generate turbulent kinetic energy (TKE) in the continuous phase

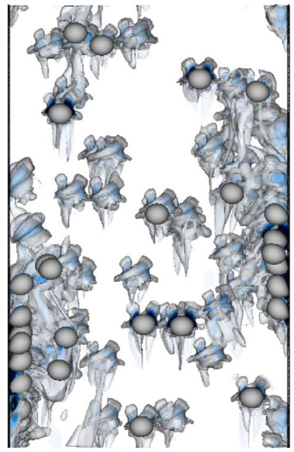

Figure 1: Instantaneous configuration of bubbles rising in a turbulent channel flow at $Re_\tau = 127$ from DNS. The flow structures are coloured according to iso-values of the so-called λ_2 criterion. Figure is adopted from [9] for a case with small spherical bubbles.

[10], see e.g. the instantaneous flow structure in Figure 1 colored by isovalues of the so-called λ_2 criterion in Direct Numerical Simulation (DNS) of [9]. If the bubbles provide the dominant source of TKE, then often referred to as the bubble-induced turbulence (BIT) regime, the success of two-equation eddy viscosity models depends, to a large extent, upon the modelling of the so-called interfacial term, S_k, that appears in the TKE equation [11, 12]. This term represents the interfacial energy transfer between the bubbles and the liquid in the TKE equation for the liquid phase derived by [13]

$$\frac{D\overline{\phi}k}{Dt} = P_k + D_k + \varepsilon_k \underbrace{- \frac{1}{\rho}\overline{p' u_i' n_i I} + \frac{1}{\rho}\overline{\tau_{ij}' u_i' n_j I}}_{S_k}, \tag{1}$$

where k is the TKE, and ϕ an indicator function for the liquid phase. The shear production term P_k, the transport term D_k, and the dissipation term ε_k have the same form as those in the corresponding single-phase flow equations, e.g. in [14]. The term S_k is an additional source term, with p', u_i', τ_{ij}' the fluctuating pressure, i-th fluctuating velocity component, and stress tensor at the liquid side of the phase boundary, respectively, and ρ is the liquid density, assumed to be constant here, throughout. Furthermore, n_i is the unit normal vector on the phase boundary that is directed toward the gas phase, and I is the interfacial area concentration with $\partial\phi/\partial x_i = -In_i$.

Despite the fact that two-equation eddy viscosity models are able to predict the TKE and the dissipation quite well, the approach suffers from substantial uncertainties concerning the eddy viscosity concept used in the Boussinesq hypothesis when applied to turbulent bubbly flows, as discussed in [15, 16]. To account for the effect of the bubbles on the eddy viscosity expression used in the equation for $\overline{\mathbf{u}}$, some authors have tried to simply vary the model constant that appears in the closures [17], while others have tried introducing additional terms to mimic the effects of the bubbles on the turbulent eddy viscosity [18]. Such approaches are similar in spirit to low-Reynolds-number (LRN) eddy viscosity models that have been applied in single-phase flow, where damping functions are introduced for C_μ and additional terms are introduced into the turbulent transport equations. The difference is that in the bubble-laden context, the modifications made are to account for the effect of the bubbles on the eddy viscosity, rather than to account for near wall effects as in LRN models.

While an eddy-viscosity, Reynolds-averaged model may be used to predict $\overline{\mathbf{u}}$ in wall-bounded flows down to the boundary, it is common for bubbly flows, just as for single-phase flows, to use wall-functions near the wall to reduce computational expense [19, 20, 21, 22, 23, 24]. However, the wall-functions used are based on those derived for single-phase flows. For example, it is assumed that in wall-bounded bubbly turbulent flows, a log-law region exists for the mean velocity, and that the bubbles simply modify the parameters in the law [25]. Such an approach may be valid for the regime $|S_k| \ll |P_k|$. However, it is not at all clear that it should apply to the BIT regime where $|S_k| \sim |P_k|$ or even $|S_k| \gg |P_k|$. Moreover, it should be noted that [25] tested their wall-function model for pipe flows where the background turbulence was strong, and the effects of the bubbles on the flow were relatively weak. Therefore, it is not clear whether the proposed bubble-modified wall-function models can be used with confidence in the BIT regime.

In practice, S_k is hard to measure directly. In experiments, S_k has been evaluated as the difference between P_k and ε_k using a simplified version of eq.(1) consisting solely of production, dissipation and interfacial terms [26]. Moreover, even in DNS studies S_k is typically estimated in a similar, indirect manner. For instance, du Cluzeau et al. [9] computed S_k as the residual in the transport equation for the Reynolds stresses. As a consequence, accurately comparing $|S_k|$ with $|P_k|$ so as to understand the energetics of the flow may be difficult. In view of this, to allow a simpler comparison across different levels of turbulence and bubble volume fractions, Rensen et al. [27] introduced the so-called 'bubblance' parameter, $b = \alpha \overline{u}_r^2 / u_0'$, where $\overline{u}_r$ is the mean relative velocity between the two phases, and u_0' is the vertical velocity fluctuation produced by the background turbulence in the absence of the bubbles. This is similar to the suggestion of [28] who used the ratio of the bubble-induced kinetic energy to the kinetic energy of the flow in the absence of the bubbles. When $b \gg 1$, the turbulence of the carrier phase is predominately produced by the motion of bubbles, whereas when $b \ll 1$, the turbulence is predominately produced by the mean shear in the flow.

The goal of the present paper is to consider the bubble-modified wall-function approach and in particular, to consider the theoretical validity of the assumption of a log-law for wall-bounded, bubbly turbulent flows in Sections 2 and 3. DNS data from previous studies is used to explore this issue.

2. Classical ansatz for deriving the log-law in single-phase flow

The log-law is widely considered to describe well many single-phase, wall bounded turbulent flows [29, 30]. As discussed in the introduction, previous studies have assumed that the log-law also applies for bubbly, wall-bounded turbulent flows. We now consider the validity of this assumption.

For simplicity, we consider the canonical case of a pressure-driven vertical turbulent plane-channel flow laden with bubbles, defined by the bulk Reynolds number $Re_b \equiv U_b 2h/\nu$, where U_b is the bulk velocity (i.e. the streamwise velocity averaged over the entire domain), h the half channel height, and ν the liquid kinematic viscosity.

In the single-phase limit, the classical theory for the mean velocity profile is based on the argument that the flow can be divided into two asymptotically defined regions, an inner region and an outer region [33]. The inner region is a region where the mean streamwise velocity in inner scales, $u^+ \equiv \overline{u}/u_\tau$, can be expressed as a function of the inner-scaled distance from the wall, $y^+ \equiv y u_\tau/\nu$, namely,

$$u^+ = f_{ui}(y^+) \ , \tag{2}$$

where $u_\tau \equiv \sqrt{\tau_w/\rho}$ is the friction velocity, τ_w the wall shear stress, ρ the liquid density, and the subscript 'ui' denotes that the function reflects $\overline{u}/u_\tau$ in the inner region. In contrast, the outer region is where the outer-scaled mean velocity, $(\overline{u}_c - \overline{u})/u_\tau$, is expressed as a function of the outer-scaled distance,

$$\frac{\overline{u}_c - \overline{u}}{u_\tau} = f_{uo}\left(\frac{y}{h}\right) \ , \tag{3}$$

where $\overline{u}_c$ is the mean centreline velocity, and the subscript 'uo' denotes that the function addresses the outer region. Defining an overlap region as a region where the inner and outer layers match, one finds that the velocity profile in the overlap region exhibits a logarithmic behaviour (see e.g. [34] or [14] for a detailed derivation), with an inner-scaled formulation

$$u^+ = \frac{1}{\kappa} \ln y^+ + B \ , \tag{4}$$

and with outer-scaled formulation

$$\frac{\overline{u}_c - \overline{u}}{u_\tau} = -\frac{1}{\kappa} \ln\left(\frac{y}{h}\right) + B_1 \ . \tag{5}$$

Here, the von Kármán constant κ is believed to be universal [35, 30] and the additive constants B and B_1 are flow dependent [36]. The results in Figure 2(a) illustrate the accuracy of this log-law when compared with data from the Princeton Superpipe experiment [31].

3. Is there a log-law for bubbly channel flows?

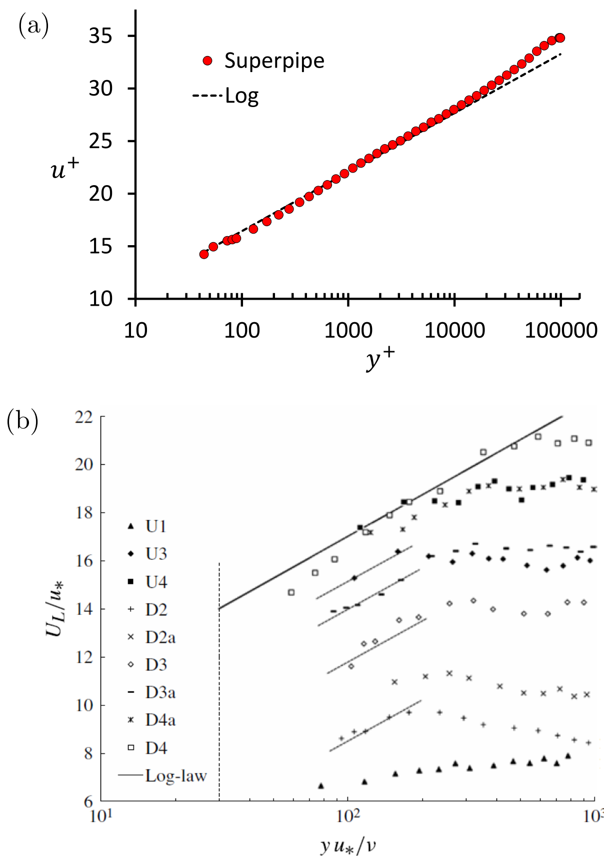

Figure 2: (a) Experimental data of the nondimensional mean streamwise velocity u^+ in a single-phase pipe flow with friction Reynolds number $Re_\tau = 98000$ [31] compared to the log-law (4). (b) Velocity distributions in bubbly pipe flows for various flow conditions (in the legend: U for upward flow, D for downward flow) compared to the log-law (Figure adopted from [32]).

3.1. Previous approach: correction function for von Karman constant

We now discuss whether a log-law may also be expected to hold for bubbly turbulent channel flows. [37] were among the first to propose a log-law for the near-wall region of bubbly flow with the same structure as eq. (4)

$$u^+ = \frac{1}{\kappa^*} \ln y^+ + B^* \ , \tag{6}$$

which involves a modified von Kármán constant $\kappa^* \equiv \kappa/\gamma$. (Note that [37] actually presented (6) in a slightly different, but equivalent form). Here, γ is a correction function that depends upon certain bubble parameters

$$\gamma \equiv \sqrt{1 - \left(\frac{g d_p}{u_\tau^2}\right)(\alpha_p - \alpha_E)} \ , \tag{7}$$

where α_p and α_E denote the near wall peak (maximum) and the free stream averaged void fraction, respectively, while d_p is the bubble diameter, and g is the gravitational acceleration. The additive constant B^* in (6) also is a function of γ.

A number of more recent studies, such as [38, 39, 40, 32] proposed differing specifications for κ^* and B^*, while still assuming the basic log-law formulation to hold (6). Table 1 in [41] lists some of the various expressions.

While several sets of experimental data have been used to support the validity of (6) for bubbly turbulent channel flow, it should be noted that almost all of these correspond to flows with high background turbulence produced by shear, and relatively little production due to the bubbles [42, 37, 43]. In particular, the levels of TKE measured in the bubble laden and the unladen cases are similar in these studies. In such a regime, it is not surprising that (6) may work well since the log-law is known to describe single-phase turbulent channel flows well. Moreover, results such as those in Figure 2(b) provide limited evidence for a log-law in bubbly turbulent channel flow, since the logarithmic fit only holds over five or six measurement points at best (see also [40] for results from a horizontal bubbly turbulent channel flow). Therefore, compared to the evidence of log-law in the single-phase case (see e.g. Figure 2a), the evidence that has been proposed for a log-law in the bubbly turbulent channel flow context is much weaker. In addition to the limited evidence for the validity of (6) for bubbly turbulent channel flow, we now point out a number of theoretical issues that seem to invalidate the idea of a log-law for the BIT regime.

3.2. Theoretical reasons why a log-law is not expected for bubbly channel flows

3.2.1. Dimensional analysis

Let us consider a fully developed single-phase channel flow, for which the mean velocity of the flow is determined by ν, h, and the mean streamwise pressure gradient $d\overline{p}/dx$. In this case, the wall-normal gradient of the streamwise velocity is given by dimensional analysis [14] as

$$\frac{d\overline{u}}{dy} = \frac{u_\tau}{y} f\Big(\frac{y}{h}, y^+\Big), \tag{8}$$

where f is supposed to be a universal, non-dimensional function. As stated earlier, the log-law can be derived by matching the inner layer asymptotic behaviour $f(y/h, y^+) \sim f_{ui}(y^+)$ to the outer layer asymptotic behaviour, $f(y/h, y^+) \sim f_{uo}(y/h)$. The crucial point, however, is that there is no reason to expect (8) to hold for bubbly turbulent channel flow. Indeed, for that case, $\overline{u}$ should depend not only on $\nu, h, d\overline{p}/dx$, but also upon bubble parameters such as the bubble diameter d_p, the local void fraction α, and the density ratio between the bubbles and fluid ρ_p/ρ_l (the subscript 'l' denotes the liquid phase and 'p' denotes the gas phase). This is because for the bubbly channel flow case, the transport equation governing $\overline{u}$ will include a term describing the momentum coupling between the bubbles and the liquid. As such, the very concept of inner and outer layers no longer makes sense, and the properties of $\overline{u}$ will now depend not only upon how pressure gradient and viscous forces compete in the liquid, but also how each of these competes with the local force due to momentum coupling between the bubbles and liquid flow.

3.2.2. Argument against log-law in form of eq. (6)

A point related to this is that it seems physically reasonable to expect that the effect of the bubbles on the flow will vary with y, a feature that is not captured by the bubble-modified log-law in (6). In particular, consider the following argument: since the eddies in the flow grow in size as y increases away from the wall, then for $Re \gg 1$, while close to the wall we may have $\ell(y) = O(d_p)$, far from the wall we may observe $\ell(y) \gg d_p$, where $\ell(y)$ describes a characteristic size of an eddy at distance y from the wall. When $\ell \gg d_p$, the eddy is so large compared to the bubble, and its typical timescale so long, that the bubble will behave almost like a tracer particle relative to the eddy, implying that the eddy will only be weakly affected by the bubbles it contains (based on typical properties of the eddies; of course there may be infrequent occasions where the energy in the eddy is small enough to be significantly affected by the bubble). By contrast, we would expect that for $\ell(y) = O(d_p)$ the bubbles are large enough to strongly affect the eddies in which they are contained. In view of this argument, one would expect that with increasing distance from the wall the effect of the bubbles on the flow would be diminished, and that in the asymptotic limit $\ell(y)/d_p \to \infty$, the flow will locally asymptote to single-phase flow behavior. If then one wishes to modify the von Kármán constant with $\kappa^* \equiv \kappa/\gamma$, then γ ought to be a function of y, so that

$$\lim_{\ell(y)/d_p \to \infty} \kappa^* \to \kappa, \tag{9}$$

is satisfied. However, if γ (and therefore κ^*) are functions of y, then (6) no longer generates a log-law for $\overline{u}$. Consequently, (6) is fundamentally inconsistent with the idea that in a high Reynolds number flow, the effect of the bubbles on the flow should diminish with distance from the wall.

The argument above only considers the properties of a single bubble, and so mainly applies when the void fraction is not too large. If the void fraction is large, then even at locations where $\ell \gg d_p$, the accumulated effect of all the bubbles may be significant enough such that the eddy is affected by the bubbles. Therefore, κ^* must depend not merely on y, but on $\alpha(y)$. A related point is that in general, BIT in a wall-bounded flow may not posses the outer region that occurs for single-phase flow. The reason is that for BIT, viscous effects are not confined to the very near wall region, but may be significant everywhere in the flow due to viscous stresses generated at the bubble surfaces.

3.2.3. location of $\overline{u}_{max}$

Finally, for single-phase flows, the maximum mean velocity $\overline{u}_{max} \equiv \max[\overline{u}]$ occurs at the center of the channel, with $\overline{u}$ a monotonically increasing function of y for $0 \leq y \leq h$. Clearly, the log-law is consistent with this monotonic behavior in the region for which it is valid. However, for bubbly turbulent flows, $\overline{u}$ depends upon the bubble void fraction, and since the bubbles may be strongly inhomogeneously distributed in the channel, $\overline{u}_{max}$ need not be located at $y = h$, but could be located anywhere in the range $0 < y \leq h$. As a result, $\overline{u}$ may vary non-monotonically with y for $0 \leq y \leq h$, inconsistent with a log-law. Some evidence for this non-monotonic behavior may be seen in Case *Sb* in Figure 12(b) of [9] and the case with $\alpha_t = 10\%$ in Figure 3 of [44].

4. Evidence from DNS that the log-law can fail for bubbly flows

Having presented arguments for why a log-law need not be expected for bubbly turbulent channel flows, we now turn to consider data from an interface-resolved DNS of such a flow. The DNS data are from [5] and [44], in which bubble-resolving DNS were conducted with many bubbles at varied Eötvös number, $Eo = \Delta\rho g d_p/\sigma$, where σ is the surface tension.

The DNSs were carried out for flow in two rectangular channels, with periodicity in the streamwise (x) and spanwise (z) directions. For upward flows, the size of the domains are $L_x \times L_y \times L_z = 2h\pi \times 2h \times h\pi$, where h is the half channel height. These are three cases (*S180, D180, D180g8*) adopted from [5], who used the code TrioCFD based on front-tracking method for two-phase flows. For two downward flows cases, the computational domain is $L_x \times L_y \times L_z = 4h\pi \times 2h \times 4/3h\pi$ (Cases *25p, 5p* in [44] based on Volume of Fluid method). These DNS data were obtained for five monodisperse cases (*S180, D180, D180g8, 25p, 5p*) with friction Reynolds number $Re_\tau = hu_\tau/\nu \approx 180$. A detailed account of the setup and the DNS methodology are provided in the original papers [5, 44]. For comparison, data from a single-phase (unladen) simulation with the same value

Parameter	*SP180*	*S180*	*D180*	*D180g8*	*25p*	*5p*
N_p	–	42	42	42	320	64
α_{tot}	–	3%	3%	3%	2.5%	0.5%
d_p/h	–	0.3	0.3	0.3	0.25	0.25
ρ_l/ρ_p	–	10	10	10	20	20
μ_l/μ_p	–	1	1	1	20	20
d_p^+	–	54	54	54	46	46
Re_τ	180	180	180	180	≈ 180	≈ 180
Re_p	–	90	140	600	$90 \sim 160$	160
Eo	–	0.45	3.6	3.6	0.67	0.67

Table 1: Parameters of the cases used for the present study according to [5] and [44]. ρ and μ represent the density and the molecular dynamic viscosity, respectively. *SP180* stands for the single-phase case with $Re_\tau = 180$, based on the results of [45]. In the bubble laden cases of [5] (*S180, D180, D180g8*), the label S is used for the cases with spherical bubbles (*S180*) and the label D for the cases with deformable bubbles (*D180, D180g8*). Cases *S180* and *D180* refer to the cases with low gravity conditions, $g = 0.1$, while *D180g8* is a case with increased gravity, $g = 0.8$. Cases *25p* and *5p* are from [44]. Furthermore, N_p is the number of bubbles, α_{tot} is the ratio of the total gas volume to the channel volume, d_p the bubble diameter, and $d_p^+ = d_p/(\nu/u_\tau)$, which is the ratio of the bubble diameter to the wall unit. The values of Re_τ, the friction Reynolds number, and Re_p, the bubble Reynolds number based on d_p and the relative velocity, are results of the simulations.

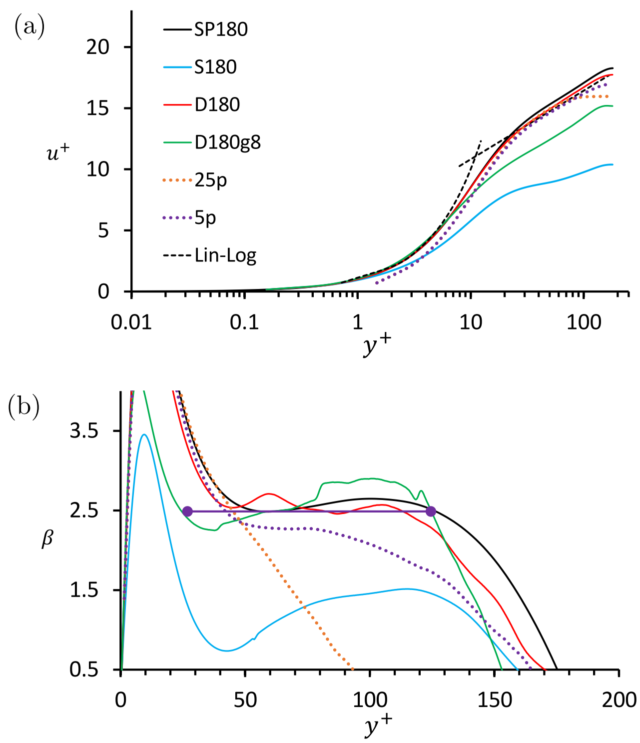

Figure 3: Assessment of logarithmic behaviour of the mean liquid velocity in bubble-laden flows (a) Velocity profile in wall units; (b) Log-law indicator function β defined in (10). The horizontal line is at $\beta = 1/\kappa$ with $\kappa = 0.4$.

of Re_τ [45] is also indicated, labelled *SP180*. Table 1 provides an overview of the parameters for the cases discussed here.

Figure 3(a) shows the mean velocity profile for all bubbly flow cases considered in Table 1, compared to the single-phase case, *SP180*. At this friction Reynolds number, the unladen case exhibits a short, but discernible approximate log layer. The results also show that some of the bubble-laden cases deviate significantly from the classical log-law, while other cases are closer to it. To examine this more carefully, in Figure 3(b) we plot

$$\beta \equiv y^+ \frac{\partial u^+}{\partial y^+} \, , \tag{10}$$

the log-law indicator function, which, in a log layer, will have a constant value equal to $1/\kappa$. With this more sensitive measure, it is clear that the mean velocity profiles for the cases *S180*, *25p*, and *5p* are not even approximately constant for any significant range of y^+ (the unladen case is also not exactly constant at this Reynolds number, but its variations from a constant value are clearly much smaller than for the bubble cases cases *S180*, *25p*, and *5p*). Cases that appeared close to a log-law in Figure 3(a), like Case *5p*, are therefore shown to be significantly different from a log-law when analysed using the more sensitive measure β. For cases *D180* and *D180g*, the curves for β are affected by statistical noise, but it appears that both cases behave similarly to the unladen case and that β may converge towards an approximately constant value between $y^+ \approx 50$ and $y^+ \approx 110$, indicating an approximate logarithmic behaviour in this region.

To explain why the mean flow profile is sometimes reasonably close to a log-law for the bubble-laden cases and at other times is far away, it is tempting to try to explain this simply in terms of the averaged void fraction α. Indeed, when $\alpha \to 0$, the unladen behaviour is recovered, possibly suggesting that in regions of the flow where α is sufficiently small, the bubble-laden channel flow may behave like the unladen case. The DNS results for α are shown in Figure 4. Note that even though most of their parameters are identical, the gas distribution of case *S180* is very different from case *D180*. The main difference between these

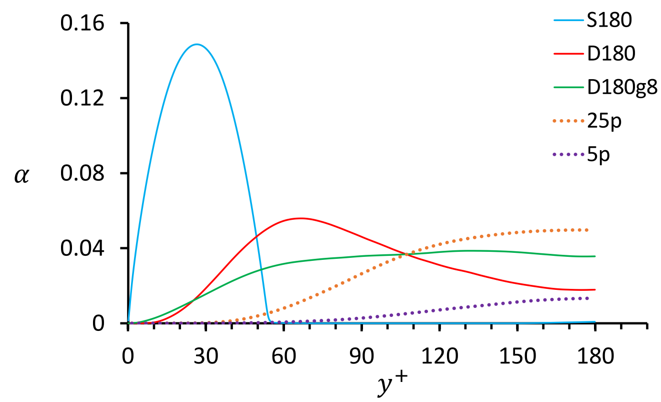

Figure 4: Profile of the averaged gas void fraction.

cases is due to their significantly different Eötvös numbers. For case S180, the bubbles are pushed towards the wall due to the lift force acting on them, and as a result the bubbles accumulate near the wall. However, the Eötvös number is considerably larger for case *D180* which leads to a reversal of the direction of the lift force so that the bubbles no longer accumulate near the wall [5]. As discussed earlier, over the region $50 < y^+ < 110$, cases *D180* and *D180g8* are relatively close to the unladen case that has an approximate log-law, whereas cases *S180*, *25p*, and *5p* are significantly different from the unladen case. Yet, the results for α in Figure 4 show that over the same region $50 < y^+ < 110$, α is considerably larger for cases *D180* and *D180g8* than it is for cases *S180*, *25p*, and *5p*. As a result, the idea that the departures from the log-law for the bubble-laden cases can be understood simply in terms of α is incorrect and overly simplistic. At present, we do not have a better explanation, except that perhaps in some cases, the effect of the void fraction is counteracted by other effects due to the bubbles, such that the mean flow profile remains relatively close to the unladen case. However, there may be some deeper underlying reason, and this must be explored in future work.

These observations are consistent with other DNS data for such flows [46, 6, 47], where the bubbles play a pivotal role in the wall-bounded flows. The experimental work of [32] claims to observe an approximate log-law for bubble-

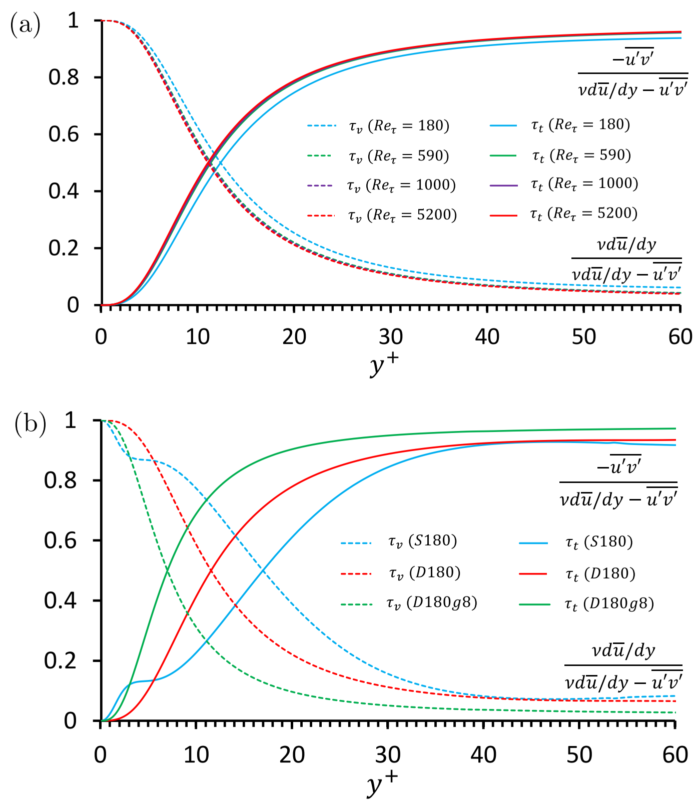

Figure 5: Profiles of the fractional contributions of the viscous and Reynolds stresses to the total stress of the continuous phase. (a) Single-phase channel flow; (b) three cases of bubbly channel flow.

laden turbulence, just as we observe for some of the present cases. In their experiments the reason the log-law was observed to approximately hold may be that in their flow the bubbles played a minor role in the flow dynamics, i.e. the dominant effect driving the flow was shear-driven turbulence, rather than bubble-induced turbulence.

In single-phase flow, different layers in the near-wall region are defined on the basis of y^+, which plays the role of a local Reynolds number, and therefore can be used as a measure of the relative importance of viscous and inertial forces at a given location in the flow. Figure 5(a) shows the fractional contributions of the viscous and Reynolds stresses to the total stress in the near-wall region of single-phase channel flows with different Re_τ. When they are plotted against y^+, the profiles for these four Reynolds numbers almost collapse (DNS data for $Re_\tau = 180$, $Re_\tau = 1000$, and $Re_\tau = 5200$ are based on the results of [45]; the data of $Re_\tau = 590$ are from [48]). The viscous contribution drops from 100% at the wall ($y^+ = 0$) to 50% at $y^+ = 12$ and is less than 10% by $y^+ = 50$. However, this behaviour is not observed for the bubbly flows considered here, as shown in Figure 5(b). In some bubble-laden cases (see *D180g8*), the Reynolds stress can increase much faster with increasing y^+ than for the single-phase case, such that the position where the Reynolds and viscous stress contributions are equal occurs below $y^+ = 10$. This difference is due to the presence of the interfacial momentum coupling term between the bubbles and the liquid that plays a key dynamic role, even very close to the wall.

The results in Figure 5(b) also show that in contrast to the single-phase case, for bubbly turbulent channel flows, the curves do not collapse (even approximately) when plotted as a function of y^+. This indicates that the wall unit $\delta_\nu = \nu/u_\tau$ no longer represents the dynamically relevant length scale near the wall when the channel flow contains bubbles. This is a manifestation of the point made earlier, namely, that for bubbly turbulent channel flows, the mean flow is not only determined by $\nu, h, d\overline{p}/dx$, but also by bubble parameters such as the bubble diameter d_p, the local void fraction α, and the density ratio ρ_l/ρ_p. A simple lengthscale based on this larger set of dynamical relevant parameters is not, however, apparent.

These results illustrate the profound effect that the bubbles can have on the turbulent flow, and why, as a consequence, a log-law need not be anticipated for the bubble-laden channel flow case. Indeed, as we have shown, it does not occur when the bubbles play a strong role in the flow dynamics.

Finally, we remind the reader that the evidence provided in the present section is based on a relatively low Reynolds number bubbly turbulent channel DNS. This is a limitation compared to log-law investigations in single-phase flows, where systematic investigations have been performed over a large range of high Reynolds number flows [30]. However, DNS data of bubbly flows with high

Re_τ are not currently available, which is mainly due to the grid requirements for interface-revolved DNS of multiphase flows, as discussed in [49]. It would be important in future work to explore the issue of the log-law for bubbly turbulent channel flows at high Re_τ when such data becomes available, in order to more thoroughly explore this topic.

5. Conclusions

We have presented theoretical arguments and evaluated results from interface-resolving DNS of bubbly turbulent channel flows demonstrating that in general, a log-law does not hold for the mean liquid velocity in the presence of the bubbles, except in regimes where the bubbles play a minor role in the flow dynamics. These departures from the log-law, that approximately hold for single-phase flow, are not surprising, even though several previous studies claimed that a log-law should hold for wall-bounded turbulent bubbly flows. The basic reason for the departures is simply that for bubbly flows, the mean flow is affected by a number of additional dynamical parameters, such as the void fraction, that are absent in the single-phase case. As a result, the inner/outer asymptotic regimes that form the basis of the derivation of the log-law for single-phase flow do not exist in general for bubbly turbulent flows. Nevertheless, we do find that for some cases, the bubbles do not cause significant departures from the log-law behaviour. However, we show that the departures cannot be understood simply in terms of the void fraction, but that more subtle effects must be playing a role.

From a modelling perspective, the importance of these results is that they show that using log-law based wall-functions in calculations of the mean liquid velocity for turbulent bubbly flows could lead to significant errors in the near wall region. To derive the equivalent of a log-law result for bubble-laden turbulent channel flow would involve replacing the inner/outer asymptotic regions used in single phase flow with some other asymptotic regions, and matching their behaviour to obtain the mean liquid flow profile. How to define these asymptotic regions is, however, at present unclear. The other approach is to build new eddy viscosity models for bubble-laden turbulent channel flow specifically designed for the near-wall region. We are currently working on this challenging area of modelling.

Finally, we note that one possible way that a log-law could emerge for wall-bounded bubbly flows is in a situation where the bubble parameters are such that all the bubbles are trapped in the very near wall region. In such a case, the bubbles would effectively produce a rough wall boundary condition on the flow, and so a log-law could still emerge for sufficiently high Reynolds numbers with the location of the log region modified to account for the roughness height, similar to what is done for single-phase turbulence in the presence of rough walls [50].

Acknowledgements

The authors are grateful to A. du Cluzeau, G. Bois, and P. Cifani for helpful discussions and providing public access to their DNS data. The data of [5] are available online (http://triocfd.cea.fr/recherche/modelisation-physique). The authors would also like to thank D. Lucas for reading the manuscript. T.M. acknowledges funding by Deutsche Forschungsgemeinschaft (DFG, German Research Foundation) under Grants MA 8408/1-1 and MA 8408/2-1.

References

[1] D. Lohse, Bubble puzzles: From fundamentals to applications, Physical Review Fluids 3 (11) (2018) 110504.

[2] D. Lucas, E. Krepper, R. Rzehak, Y. Liao, T. Ma, T. Ziegenhein, Status and challenges of cfd-modelling for poly-disperse bubbly flows, in: NURETH-16: Proceedings of the 16th International Topical Meeting on Nuclear Reactor Thermal Hydraulics, 2015.

[3] T. Ma, A contribution to turbulence modelling in bubbly flows, Ph.D. thesis, Institute of Fluid Mechanics, Technische Universität Dresden, TUD-press Verlag der Wissenschaften GmbH, Dresden. (2017).

[4] J. Lu, G. Tryggvason, Effect of bubble deformability in turbulent bubbly upflow in a vertical channel, Phys. Fluids 20 (2008) 040701.

[5] A. du Cluzeau, G. Bois, A. Toutant, J.-M. Martinez, On bubble forces in turbulent channel flows from direct numerical simulations, J. Fluid Mech. 882 (2020) A27.

[6] C. Santarelli, J. Fröhlich, Direct numerical simulations of spherical bubbles in vertical turbulent channel flow. Influence of bubble size and bidispersity, Int. J. Multiphase Flow 81 (2016) 27–45.

[7] X. Chu, Y. Liu, W. Wang, G. Yang, B. Weigand, H. Nemati, Turbulence, pseudo-turbulence, and local flow topology in dispersed bubbly flow, Physics of Fluids 32 (8) (2020) 083310.

[8] J. Lu, G. Tryggvason, Multifluid flows in a vertical channel undergoing topology changes: Effect of void fraction, Physical Review Fluids 4 (8) (2019) 084301.

[9] A. du Cluzeau, G. Bois, A. Toutant, Analysis and modelling of reynolds stresses in turbulent bubbly up-flows from direct numerical simulations, J. Fluid Mech. 866 (2019) 132–168.

[10] T. Ma, B. Ott, J. Fröhlich, A. D. Bragg, Scale-dependent anisotropy, energy transfer and intermittency in bubble-laden turbulent flows, J. Fluid Mech. in press (2021).

[11] M. Wörner, S. Erdogan, Toward improved closure relations for the turbulent kinetic energy equation in bubble-driven flows, Chemie Ingenieur Technik 85 (7) (2013) 1131–1136.

[12] T. Ma, C. Santarelli, T. Ziegenhein, D. Lucas, J. Fröhlich, Direct numerical simulation-based Reynolds-averaged closure for bubble-induced turbulence, Phys. Rev. Fluids 2 (2017) 034301.

[13] I. Kataoka, A. Serizawa, Basic equations of turbulence in gas-liquid two-phase flow, Int. J. Multiphase Flow 15 (1989) 843–855.

[14] S. B. Pope, Turbulent Flows, 1st Edition, Cambridge University Press, 2000.

[15] T. Ma, D. Lucas, A. D. Bragg, Explicit algebraic relation for calculating reynolds normal stresses in flows dominated by bubble-induced turbulence, Phys. Rev. Fluids 5 (2020) 084305.

[16] T. Ma, D. Lucas, S. Jakirlić, J. Fröhlich, Progress in the second-moment closure for bubbly flow based on direct numerical simulation data, J. Fluid Mech. 883 (2020).

[17] B. Magolan, E. Baglietto, Assembling a bubble-induced turbulence model incorporating physical understanding from dns, Int. J. Multiphase Flow 116 (2019) 185–202.

[18] M. L. de Bertodano, R. T. Lahey, O. C. Jones, Development of a k-epsilon model for bubbly two-phase flow, Journal of Fluids Engineering 116 (1994) 128.

[19] M. Colombo, M. Fairweather, Multiphase turbulence in bubbly flows: RANS simulations, Int. J. Multiphase Flow 77 (2015) 222–243.

[20] T. Ma, D. Lucas, T. Ziegenhein, J. Fröhlich, N. Deen, Scale-Adaptive Simulation of a square cross-sectional bubble column, Chem. Eng. Sci. 131 (2015) 101–108.

[21] T. Ziegenhein, R. Rzehak, T. Ma, D. Lucas, Towards a unified approach for modelling uniform and non-uniform bubbly flows, Can. J. Chem. Eng. 95 (1) (2017) 170–179.

[22] L. Liu, O. Keplinger, T. Ma, T. Ziegenhein, N. Shevchenko, S. Eckert, H. Yan, D. Lucas, Euler-euler simulation and x-ray measurement of bubble chain in a shallow container filled with liquid metals, Chem. Eng. Sci. 192 (2018) 288–305.

[23] Y. Liao, T. Ma, L. Liu, T. Ziegenhein, E. Krepper, D. Lucas, Eulerian modelling of turbulent bubbly flow based on a baseline closure concept, Nucl. Eng. Des. 337 (2018) 450 – 459.

[24] Y. Liao, T. Ma, E. Krepper, D. Lucas, J. Fröhlich, Application of a novel model for bubble-induced turbulence to bubbly flows in containers and vertical pipes, Chem. Eng. Sci. 202 (2019) 55–69.

[25] A. A. Troshko, Y. A. Hassan, Law of the wall for two-phase turbulent boundary layers, International journal of heat and mass transfer 44 (4) (2001) 871–875.

[26] J. Lelouvetel, T. Tanaka, Y. Sato, K. Hishida, Transport mechanisms of the turbulent energy cascade in upward/downward bubbly flows, J. Fluid Mech. 741 (2014) 514–542.

[27] J. Rensen, S. Luther, D. Lohse, The effect of bubbles on developed turbulence, J. Fluid Mech. 538 (2005) 153–187.

[28] M. Lance, J. Bataille, Turbulence in the liquid phase of a uniform bubbly air-water flow, J. Fluid Mech. 222 (1991) 95–118.

[29] A. J. Smits, B. J. McKeon, I. Marusic, High–reynolds number wall turbulence, Annu. Rev. Fluid Mech. 43 (2011).

[30] I. Marusic, J. P. Monty, M. Hultmark, A. J. Smits, On the logarithmic region in wall turbulence, Journal of Fluid Mechanics 716 (2013).

[31] M. Hultmark, M. Vallikivi, S. C. C. Bailey, A. J. Smits, Turbulent pipe flow at extreme reynolds numbers, Phys. Rev. Lett. 108 (9) (2012) 094501.

[32] C. Colin, J. Fabre, A. Kamp, Turbulent bubbly flow in pipe under gravity and microgravity conditions, J. Fluid Mech. 711 (2012) 469–515.

[33] C. B. Millikan, A critical discussion of turbulent flow in channels and circular tubes, in: Proc. 5th Int. Congress on Applied Mechanics (Cambridge, MA, 1938), Wiley, 1939, pp. 386–392.

[34] H. Tennekes, J. L. Lumley, A first course in turbulence, MIT press, 1972.

[35] E.-S. Zanoun, F. Durst, H. Nagib, Evaluating the law of the wall in two-dimensional fully developed turbulent channel flows, Physics of Fluids 15 (10) (2003) 3079–3089.

[36] I. Marusic, B. J. McKeon, P. A. Monkewitz, H. M. Nagib, A. J. Smits, K. R. Sreenivasan, Wall-bounded turbulent flows at high reynolds numbers: recent advances and key issues, Phys. Fluids 22 (6) (2010) 065103.

[37] J. Marie, E. Moursali, S. Tran-Cong, Similarity law and turbulence intensity profiles in a bubbly boundary layer at low void fractions, Int. J. Multiphase Flow 23 (2) (1997) 227–247.

[38] C. Gabillet, C. Colin, J. Fabre, Experimental study of bubble injection in a turbulent boundary layer, Int. J. Multiphase Flow 28 (4) (2002) 553–578.

[39] S. Tran-Cong, J.-L. Marié, R. J. Perkins, Bubble migration in a turbulent boundary layer, Int. J. Multiphase Flow 34 (8) (2008) 786–807.

[40] F. Ramstorfer, H. Steiner, G. Brenn, Effect of the vapor phase on the near-wall velocity field in subcooled boiling flow, in: Proccedings of the 6th International Conference on Multiphase Flow, 2007.

[41] Y. A. Hassan, Multi-scale full-field measurements and near-wall modeling of turbulent subcooled boiling flow using innovative experimental techniques, Nucl. Eng. Des. 299 (2016) 46–58.

[42] T. Liu, S. Bankoff, Structure of air-water bubbly flow in a vertical pipe—i. liquid mean velocity and turbulence measurements, International Journal of Heat and Mass Transfer 36 (4) (1993) 1049–1060.

[43] M. Shawkat, C. Ching, M. Shoukri, Bubble and liquid turbulence characteristics of bubbly flow in a large diameter vertical pipe, Int. J. Multiphase Flow 34 (8) (2008) 767–785.

[44] P. Cifani, J. Kuerten, B. Geurts, Flow and bubble statistics of turbulent bubble-laden downflow channel, International Journal of Multiphase Flow 126 (2020) 103244.

[45] M. Lee, R. D. Moser, Direct numerical simulation of turbulent channel flow up to $Re_\tau \approx 5200$, J. Fluid Mech. 774 (2015) 395–415.

[46] S. Dabiri, J. Lu, G. Tryggvason, Transition between regimes of a vertical channel bubbly upflow due to bubble deformability, Phys. Fluids 25 (2013) 102110.

[47] P. Cifani, J. Kuerten, B. Geurts, Highly scalable dns solver for turbulent bubble-laden channel flow, Comput. Fluids 172 (2018) 67–83.

[48] A. W. Vreman, J. G. M. Kuerten, Statistics of spatial derivatives of velocity and pressure in turbulent channel flow, Phys. Fluids 26 (8) (2014) 085103.

[49] S. Subramaniam, Multiphase flows: Rich physics, challenging theory, and big simulations, Physical Review Fluids 5 (11) (2020) 110520.

[50] K. A. Flack, M. P. Schultz, Roughness effects on wall-bounded turbulent flows, Physics of Fluids 26 (10) (2014) 101305.